Chinese Journal of
POLYMER SCIENCE

RESEARCH ARTICLE

https://doi.org/10.1007/s10118-023-3049-5
Chinese J. Polym. Sci. **2024**, *42*, 407–416

Spherical Confinement Generates Entropic Force to Accelerate Polymer Chain Detachment

Yu-Shan Zheng, Jian-Ping Zhou, Yan Xu*, and Kai Li*

Mechanical Engineering, Xinjiang University, Urumqi 830002, China

Abstract To understand the dynamic process of polymer detachment, it is necessary to determine the mean detachment time of a single breakable link, which is modeled as a spring. Normally, this time can be viewed as the escape of a Brownian particle from the potential well of the spring. However, as the free dangling length of the polymer chain increases, the conformational entropy of the chain is affected by geometric confinement. It means that the wall exerts a repulsive force on the chain, resulting in accelerated link detachment from a macroscopic perspective. In this work, we investigate the effect of entropy on the detachment rate in the case where the substrate is spherical. We demonstrate that spherical confinement accelerates chain detachment both inside and outside the sphere. An analytical expression for the mean detachment time of breakable links is given, which includes an additional pre-factor that is related to the partition function. Additionally, we analyze the expressions for entropic forces inside the sphere, outside the sphere, and on a flat wall, comparing their magnitudes to explain the difference in mean detachment time.

Keywords Polymer detachment; Breakable link; Entropic force; Mean first passage time

Citation: Zheng, Y. S.; Zhou, J. P.; Xu, Y.; Li, K. Spherical confinement generates entropic force to accelerate polymer chain detachment. *Chinese J. Polym. Sci.* **2024**, *42*, 407–416.

INTRODUCTION

Polymer detachment from surface adsorption is a common phenomenon in biological systems and is essential for maintaining the activities of life.[1–7] Examples of this include bundles of F-actin, which are cross-linked with various types of sticky molecules,[3] and biopolymers that are attached to the membrane of cells or vesicles.[8–10] Single molecule manipulation techniques have facilitated the study of detachment of long macromolecules from substrates of different types. Experimental results obtained through these techniques provide fine-grained details of the detachment process at the microscopic level,[11–13] such as the critical force required for breaking base pairs during DNA separation[14,15] and the detachment rate of polymer chains from the surface.[16–18] In order to fully understand these biophysical phenomena or quantify the results of experiments, it is often necessary to conduct theoretical investigations of the process of polymer detachment from the substrate. Such investigations can provide crucial insights into the underlying mechanisms of detachment and help researchers develop predictive models for experimental outcomes.

Typically, the binding potential in polymer detachment studies is realized through explicitly discrete breakable links,[19,20] where the binding energy of each link ranges from approximately one k_BT (hydrogen bonds) to tens of k_BT (covalent bonds).[20] Most theoretical studies of polymer detachment focus on equilibrium statistical thermodynamics, simplifying the process into two states (fully adsorbed and fully detached).[14,16,21–23] However, detachment is essentially a kinetic process that involves various reactions before the molecule is fully detached. Describing the evolution of the entire system thus requires a set of kinetic equations. To derive these equations, it is necessary to determine the mean detachment time of individual breakable links.

The breakable link in polymer detachment studies is typically modeled as a spring,[24,25] and its mean detachment time can be projected as a one-dimensional problem in which a Brownian particle escapes from the spring potential well.[26] The presence of an applied force tends to tilt the potential energy landscape, resulting in a lower barrier that significantly affects the detachment time of the link. Such forces include mechanical forces, electric field forces, *etc*.[27–30] A special type of force also arises from an entropic repulsion between the wall and the free-moving end of the chain called the entropic force. In the most common case, a hard flat substrate causes reduction of polymer chain configurations, which accelerates the detachment of the adsorbed polymer chains.[26,31,32]

The entropic repulsion between the wall and the free-moving end of the chain is affected by the roughness of substrate surfaces and exhibits a rich behavior that can impact the de-

* Corresponding authors, E-mail: lilixiu_z@163.com (Y.X.)
E-mail: likai@xju.edu.cn (K.L.)

Received August 15, 2023; Accepted August 31, 2023; Published online September 27, 2023

tachment process. For example, the adsorption-desorption transition of a polymer on a curved surface occurs at a lower transition temperature,[33] and a higher degree of roughness of the surface induces stronger polymer adsorption.[34] However, little is known about the curvature dependence of the mean detachment time of a breakable link with one end tethered to a polymer chain. Complex interfaces, especially spherical surfaces, are worthy of study since cells and vesicles are typically modeled as spheres for investigation.[2,35,36] The curvature dependence of polymer entropy significantly changes the rupture rate of breakable links and should be incorporated into theoretical investigations to gain a deeper understanding of the underlying mechanisms governing polymer detachment from curved surfaces.

In this work, we present a theoretical analysis of the mean detachment time of a specific link under spherical confinement. This quantity depends on various factors such as the length of the chain, the radius of the sphere, and the spring constant. We use the mean first passage time (MFPT) technique[37,38] to calculate the mean detachment time of a breakable link that is tethered to a polymer chain without re-connecting. This technique estimates the time it takes for a particle to reach the boundary of a given domain. In our model, the domain is modelled by a potential well that incorporates the spring potential and the entropy effect. The mean detachment time of the link corresponds to the time it takes for the diffusing particle to reach the local maximum of the potential well and can be solved theoretically.

This study is organized as follows. In Section **TOY MODEL AND EFFECTIVE POTENTIAL**, we discuss the expressions for the effective potential energy. This energy includes the spring potential energy and the entropy effect along the unbinding coordinate. We present an analytical expression for the effective potential energy inside and outside the sphere. In Section **MEAN DETACHMENT TIME $\tau^{\pm}$ OF THE BREAKABLE LINK**, we introduce the MFPT method to find the mean detachment time of the breakable link in this context. We also show that the difference in detachment time inside and outside the sphere, which is due to a pre-factor related to the partition function of the polymer in confinement. In Section **INVESTIGATIONS OF ENTROPIC FORCE**, we analyze the difference in the mean detachment time of the link inside and outside the spheres starting from the entropic forces due to geometric confinement. Finally, we provide a conclusion and discuss the main results of our study.

TOY MODEL AND EFFECTIVE POTENTIAL

Effective Potential Energy Contributed by the Entropic Effect

To investigate the detachment of polymer chains under spherical confinement, we chose to model the system using the Gaussian chain model and a rigid sphere with radius R as shown in Fig. 1. In the Gaussian chain model, the length of the chain can be written as $L = Nb$, which consists of N segments, each of length b (Kuhn or monomer length). One end of the chain is anchored to a breakable link, which is simplified by a spring with spring constant k and initial length l. We define ξ as the spring's elongation and restrict it in the radius direction of the sphere.

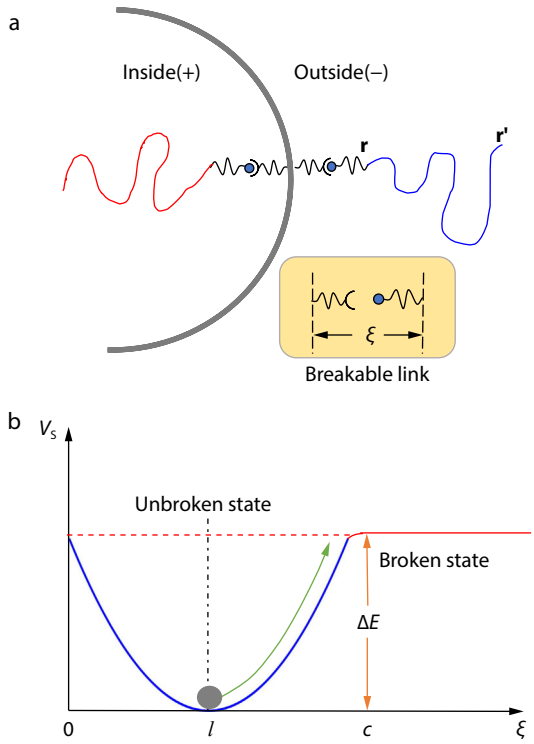

Fig. 1 (a) The schematic diagram of one breakable link tethered a Gaussian chain attached to surface inside or outside the sphere. The detached chain free to fluctuate with one end at **r** and the other end at **r'**; (b) The detachment of the link can be projected as the Brownian particle escapes from the spring potential well without considering entropy effect.

The spring potential energy can be expressed as $k(\xi - l)^2/2$ (see Fig. 1b). The other end of the chain satisfies a certain probability distribution in space due to the Brownian fluctuations. The link breaks when the elongation of spring reaches the link-breaking distance $\xi = c$. We do not consider a possible re-connecting as we are only interested in finding the detachment time.

In our system, the tethered chain segments freely explore the confined space, subject to thermal motion and spring constraint. The confinement reduces the configuration of polymer chains compared to free space, resulting in additional potential energy due to the entropy effect. The effective potential:

$$V = V_S + V_E \tag{1}$$

is the combination of a spring potential V_S and an entropic contribution V_E. Where V_E is related to the distribution function of the entire Gaussian chain under the geometric confinement:

$$V_E^{\pm} = -k_B T \ln Z^{\pm} \tag{2}$$

$Z^{\pm}$ is the reduced partition function of the Gaussian chain. The reference state is chosen as a same polymer in free space since V_E is only related to entropy effect of the Gaussian chain. The plus and minus signs represent the chain confined inside and outside the sphere, respectively. The partition function represents the sum of all conformations of the polymer with one end at **r** and the other end at **r'** that are satisfied with the externally imposed boundary conditions. It can be obtained by integrating the Green's function as:[25,39]

https://doi.org/10.1007/s10118-023-3049-5

$$Z^{\pm} = \frac{1}{V_0^{\pm}} \int \mathrm{d}\mathbf{r}\mathrm{d}\mathbf{r}' G^{\pm}(\mathbf{r}, \mathbf{r}', N) \tag{3}$$

where $V_0^{\pm}$ represents the system volume. The Green's function $G^{\pm}(\mathbf{r},\mathbf{r}',N)$ represents the probability of a Gaussian chain with the number of chain segments N, with one end at $\mathbf{r}$ and another end at $\mathbf{r}'$. If the excluded volume effects are not considered, the Green's function $G(\mathbf{r},\mathbf{r}',N)$ satisfies the diffusion equation:[40]

$$\frac{\partial G(\mathbf{r}, \mathbf{r}', N)}{\partial N} = \frac{b^2}{6} \nabla_{\mathbf{r}}^2 G(\mathbf{r}, \mathbf{r}', N) \tag{4}$$

with the initial condition $G(\mathbf{r},\mathbf{r}',N) = \delta(\mathbf{r}' - \mathbf{r})$ at N=0, and the impenetrability condition due to the sphere can be represented by the boundary conditions:

$$G^{\pm}(\mathbf{r}, \mathbf{r}', N)\big|_{\mathbf{r}'=R} = 0 \tag{5}$$

In the absence of external potential energy, the Green's function in Eq. (4) satisfies a Gaussian distribution with variance $Nb^2/3$ as follows:

$$G(\mathbf{r}, \mathbf{r}', N) \propto \exp\left[-3(\mathbf{r} - \mathbf{r}')^2 / 2Nb^2\right] \tag{6}$$

Integrating the Green's function by combining Eqs. (3) and (4) yields a partition function Z=1, which implies that V_E=0 in Eq. (1). In this case, the mean detachment time of the link is only related to the spring potential energy and can be seen as the escape of a single Brownian particle from the potential well $V = k(\xi - l)^2/2$.

However, when a Gaussian chain is subjected to geometric confinement, we need to consider the effect of entropy on the detachment process. Specifically, the detached chain strongly prefers not to touch the sphere surface and gives rise to an entropic repulsive force. To account for this effect, we first need to derive the expressions for the Green's functions of the Gaussian chain inside and outside the sphere. In the next subsection, we will provide the expressions for the Green's functions in each case and compare the effective potential for polymer detachment inside and outside the sphere.

Effective Potential under Spherical Confinement

In this Section, we consider how the spherical confinement exerts an entropic repulsion and changes the initial elastic potential energy. Solving the diffusion equation Eq. (4) under boundary conditions Eq. (5) can obtain the Green's function of the polymer chains tethered to the inside and outside surfaces of the sphere:[41–44]

$$G^{+}(\mathbf{r}, \mathbf{r}', N) = \frac{1}{2\pi R^2 \sqrt{rr'}} \sum_{n=0}^{\infty} \sum_{\beta} (2n+1) P_n(\cos\gamma) \frac{J_{n+(1/2)}\left(\beta \frac{r}{R}\right) J_{n+(1/2)}\left(\beta \frac{r'}{R}\right)}{\left[J'_{n+(1/2)}(\beta)\right]^2} \exp\left(-\frac{\beta^2 Nb^2}{6R^2}\right) \tag{7}$$

$$G^{-}(\mathbf{r}, \mathbf{r}', N) = \frac{1}{4\pi\sqrt{rr'}} \sum_{n=0}^{\infty} (2n+1) P_n(\cos\gamma) \int_0^{\infty} \frac{C_{n+(1/2)}(ur) C_{n+(1/2)}(ur')}{J_{n+(1/2)}^2(uR) + Y_{n+(1/2)}^2(uR)} \exp\left(-\frac{Nb^2 u^2}{6}\right) u\mathrm{d}u \tag{8}$$

where γ is the angle between the two vectors $\mathbf{r}$ and $\mathbf{r}'$ from the origin of the spherical cavity, $P_n(\cos\gamma)$ are the Legendre polynomials of order n, J_v and Y_v are the Bessel functions of the first and second kind of order v, and β is the positive roots of $J_{n+(1/2)}(\beta)$=0. $C_{n+(1/2)}$ is defined by $J_{n+(1/2)}$ and $Y_{n+(1/2)}$ as:

$$C_{n+(1/2)}(z) = J_{n+(1/2)}(z) Y_{n+(1/2)}(uR) - Y_{n+(1/2)}(z) J_{n+(1/2)}(uR) \tag{9}$$

The polymer chain has a free fluctuating end, while the tethered end with a spring is limited to moving along the radial direction. The origin of the coordinate is set in the center of the sphere, and the tethered end inside and outside the sphere can be expressed as $R - \xi$ and $R + \xi$. By averaging over all possible locations of the free end, we can obtain the partition functions of the chain inside and outside the sphere[43,44] (see **APPENDIX** for detailed process):

$$\begin{aligned} Z^{+}(\xi) &= \int_0^{2\pi} \mathrm{d}\phi \int_0^{\pi} \mathrm{d}\gamma \sin(\gamma) \int_0^{R} r'^2 \mathrm{d}r' G^{+}(r, r', N) \\ &= \frac{2R}{\pi(R-\xi)} \sum_{m=1}^{\infty} \frac{(-1)^{m+1}}{m} \sin\left[\frac{m\pi(R-\xi)}{R}\right] \\ &\quad \times \exp\left[-\frac{m^2\pi^2 R_g^2}{R^2}\right] \end{aligned} \tag{10}$$

$$\begin{aligned} Z^{-}(\xi) &= \int_0^{2\pi} \mathrm{d}\phi \int_0^{\pi} \mathrm{d}\gamma \sin(\gamma) \int_R^{\infty} r'^2 \mathrm{d}r' G^{-}(\mathbf{r}, \mathbf{r}', N) \\ &= \frac{\xi + R \cdot \mathrm{erf}\left(\xi / 2R_g\right)}{R + \xi} \end{aligned} \tag{11}$$

where erf(x) is the error function, and $R_g^2 = \frac{Nb^2}{6}$ is the radius of gyration of the Gaussian chain.

The expression of the series in Eq. (10) can usually retain only the first term when the chain is very long (Nb^2>>R). For the case of a relatively large sphere radius (R>>ξ), Eq. (11) degenerates to obtain the partition function under the flat wall confinement by the 'image' principle method.[42] At large spring length, the partition function Z^- tends to 1 and $V_E^- = 0$, which implies that an entropic repulsion is only observed near the wall outside the sphere.

Combining Eqs. (1), (10) with (11), we get the effective potential energy analytical solution as:

$$V^{\pm}(\xi) = \frac{k}{2}(\xi - l)^2 - k_B T \ln\left[Z^{\pm}(\xi)\right] \tag{12}$$

In biological systems, the initial length of the spring l is usually of the same magnitude as the segment length b. In our model, we set l=b=2 nm at room temperature. Typically, the link breaking distance c is normally 2 to 3 times the initial length and we assumed c=4 nm. The characteristic link binding energy usually ranges from 5 k_BT to 20 k_BT depending on the type of interaction[20,45,46] and we choose the appropriate spring factor $k(c - l)^2/2$=5k_BT.

Then Figs. 2(a) and 2(b) show the potential heights (difference between potential minimum and right side potential maximum) and the position of the potential minima as a function of N and R. It can be observed that the variation of potential energy is more obvious when N and R are small. Here, we choose the variation of potential energy with ξ corresponding to N=1, 3, 50 in Fig. 2(c). Gaussian chains are typically chosen to calculate long chains, and it is not realistic to see short chains with N=1 or 3. We choose short chains only for theoretical analysis, which differs from reality. We first give the spring potential well without considering the effect of entropy (black solid line). The chain length was then continuously increased by changing the number of segments N. The

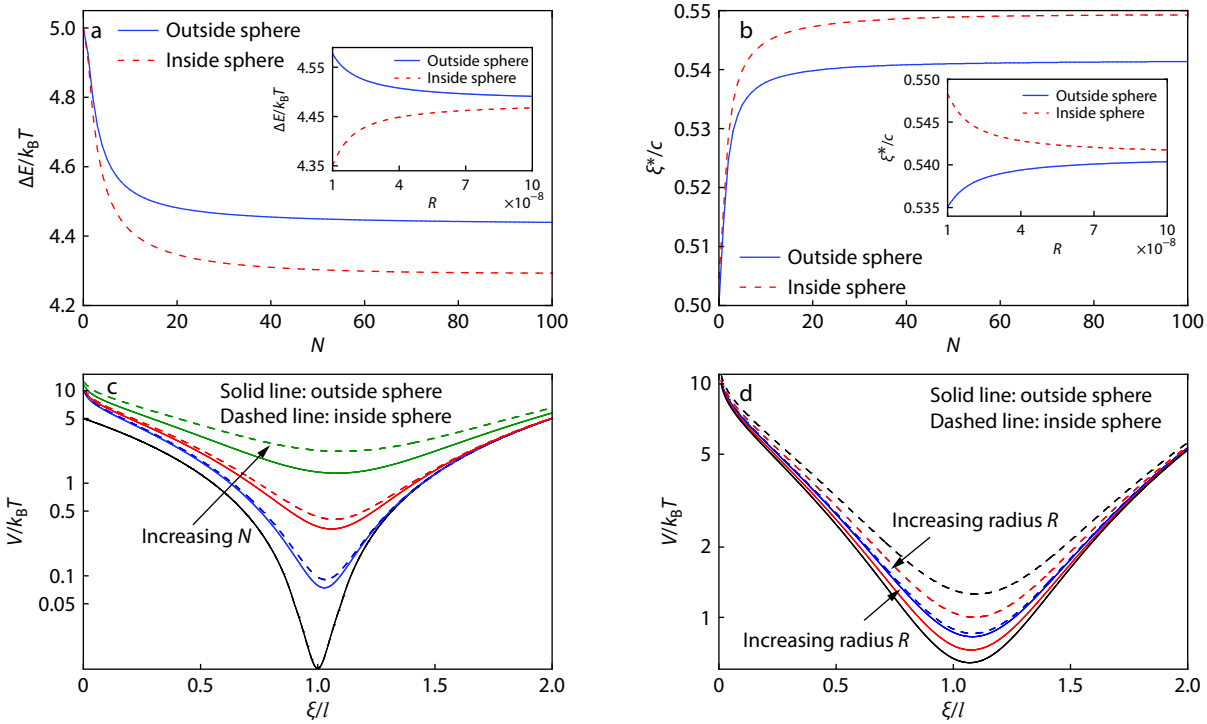

Fig. 2 The barrier height ΔE (a) and the position of the potential minimum ξ^* (b) as the function of the number of chain segments N and the sphere radius R. We set R=20 nm (main figure) and N=10 (inset) in (a) and (b). Plot of the dimensionless effective potential V against dimensionless spring length ξ/l, with different chain segments (c) and sphere radius (d). In plot (c), the black line represents the spring potential well without entropy effect. The radius of the sphere is set R=20 nm. The other lines indicate detached chains with different chain segments as N=1 (blue), 3 (red), and 50 (green). And in plot (d), the number of detached chain segments is set to N=10, and the sphere radius R=10 nm nm (black), 20 nm (red), and 100 nm (blue) increase in the direction of arrow.

chain length increasing leads to a stronger entropic repulsion, which is intuitively shown as tilting the potential energy landscape. The minimum of effective potential moves farther away from the equilibrium chain segment length as a result of V_E. It is also found that the link inside the sphere (dashed lines) is more likely to rupture for the same chain length, sphere radius, and spring constant. We also compare the effective potential energy in the case of confining inside and outside the sphere under different sphere radius (see Fig. 2d). The minimum of effective potential inside the sphere decreases as the radius increases while the potential energy outside the sphere becomes greater. They converge to a stable value as the radius large enough (approximation to flat wall confinement).

In this subsection, we provide an analytical expression for the effective potential energy of a single link under spherical confinement with one end tethered to a polymer chain. Neglecting the excluded volume effects, the entropic contribution to the potential energy is related to the partition function of the confined Gaussian chain. The spherical confinement creates a repulsive force that lowers the energy barrier for chain's detachment and accelerates the process. Differences in the partition functions of Gaussian chains inside and outside the sphere lead to distinct potential energy landscapes and result in varying detachment times for the breakable link. We will calculate and discuss these detachment times in the next section.

MEAN DETACHMENT TIME $\tau^{\pm}$ OF THE BREAKABLE LINK

The mean detachment time of the breakable link can be regarded as the time for the particle to escape from the potential well. In this work, we use the well-known MFPT technique in statistical mechanics to estimate the time $\tau^{\pm}$ for the link to be stretched from its initial length l to length c and broken. We project the detachment system into a Brownian particle that reaches the right-hand maximum from near the bottom of the effective potential energy $V^{\pm}(\xi)$, which is a simple one-dimensional problem. We assume there is a reflecting boundary condition at ξ=0 and an absorbing boundary condition at $\xi = c$ (re-connecting of the link is not considered in this article). The MFPT of the system satisfied:[38,47,48]

$$\mathcal{L}_{FP}^{\dagger}\tau(\xi) = -1 \tag{13}$$

where $\mathcal{L}_{FP}^{\dagger}$ is the backward Fokker-Planck operator:

$$\mathcal{L}_{FP}^{\dagger} = A(\xi)\frac{d}{d\xi} + B(\xi)\frac{d^2}{d\xi^2} \tag{14}$$

where the drift term is determined by the external potential $V(\xi)$ in the form of $A = -V'(\xi)/\mu$ (μ being the drag constant). Moreover, the diffusion coefficient is a strictly positive function $B = D = k_BT/\mu$. In order to calculate the MFPT, we need to solve the differential equation:

$$\left(A(\xi)\frac{d}{d\xi} + B(\xi)\frac{d^2}{d\xi^2}\right)\tau = -1 \tag{15}$$

To solve this equation, we define the function $\Psi(\xi)$ through $\Psi'(\xi) = A(\xi)/B(\xi)$ to write Eq. (15) in the form:

$$\{\exp[\Psi(\xi)]\tau'(\xi)\}' = -\frac{1}{D}\exp[\Psi(\xi)] \tag{16}$$

with the boundary conditions, the general solution of Eq. (16) is obtained after two integrations:

$$\begin{aligned}\tau(\xi) = &-\frac{1}{D}\int_0^{\xi}\exp[-\Psi(z)]\mathrm{d}z\int_0^{z}\exp[\Psi(y)]\mathrm{d}y\\ &+\omega_1\int_0^{\xi}\exp[-\Psi(y)]\mathrm{d}y+\omega_2\end{aligned} \tag{17}$$

where the constants ω_1 and ω_2 are to be determined from the boundary conditions. For the reflecting boundary condition at ξ=0, $\tau(\xi)$ satisfies $(\mathrm{d}\tau/\mathrm{d}\xi)_{\xi=0}$=0. And for the absorbing boundary condition located at ξ=c, $\tau(\xi)$ satisfies $\tau(c)$=0, we can obtain:

$$\omega_1 = 0, \omega_2 = \frac{1}{D}\int_0^{c}\exp[-\Psi(z)]\,\mathrm{d}z\int_0^{z}\exp[\Psi(y)]\,\mathrm{d}y \tag{18}$$

Substituting ω_1, ω_2 and $\Psi(\xi) = -V(\xi)/k_BT$ into Eq. (17), we get:

$$\tau^{\pm}(\xi) = \frac{1}{D}\int_{\xi}^{c}\exp\left[\frac{V^{\pm}(z)}{k_BT}\right]\mathrm{d}z\left\{\int_0^{z}\exp\left[-\frac{V^{\pm}(y)}{k_BT}\right]\mathrm{d}y\right\} \tag{19}$$

Note that D is a relevant parameter that would not cause any errors and is chosen as a constant (1 nm·s^{-2}) for convenience in calculation throughout the remainder of this work.

The integral within the brackets in Eq. (19) can typically be solved by the saddle-point method. For example, the saddle point corresponding to the effective potential energy of the Gaussian chain outside the sphere is given by the following equation:

$$(\xi^* - l) = \frac{k_BT}{k}\left[\frac{1+R\cdot\exp\left(-\xi^{*2}/4R_g^2\right)/\sqrt{\pi}R_g}{R\mathrm{erf}\left(\xi^*/2R_g\right)+\xi^*} - \frac{1}{R+\xi^*}\right] \tag{20}$$

where ξ^* is the saddle point and is difficult to solve analytically because of the error function in Eq. (20).

The saddle point in Eq. (20) can be approximated with a large spring constant k. This is reasonable for a real biopolymer system above 5 k_BT. Fig. 2(c) shows that the saddle point converges to a constant value in the long chain limit. Under the large-k assumption and long chain limit, we can simplify our calculation by taking the saddle point $\xi^*\approx1$ instead of solving Eq. (20) directly. Additionally, since the internal exponential function decays rapidly away from the saddle point, we can replace the upper limit of inside integration with ∞. Now the inside integral of the variable y in curly brackets can be expressed as:

$$\begin{aligned}&\int_0^{z}\exp\left[-V^{-}(y)/k_BT\right]\mathrm{d}y\\ &\approx Z^{-}(l)\int_0^{\infty}\exp\left[-k(y-l)^2/2k_BT\right]\mathrm{d}y\\ &= Z^{-}(l)\sqrt{\frac{\pi k_BT}{2k}}\left[1+\mathrm{erf}\left(l\sqrt{\frac{k}{2k_BT}}\right)\right]\end{aligned} \tag{21}$$

In our model, the link begins to detach from the surface of the sphere at the minimum potential energy position $\xi = l$. Therefore, the lower limit of the second integral outside the brackets related to z in Eq. (19) should be replaced with l. It is noteworthy that the major contribution of this integral is around $\xi = c$. Consequently, we can replace $Z^{-}(z)$ in the effective potential with $Z^{-}(c)$, which allows us to analytically calculate the integral:

$$\begin{aligned}&\int_l^{c}\exp\left[V^{-}(z)/k_BT\right]\mathrm{d}y\\ &\approx\frac{1}{Z^{-}(c)}\int_l^{c}\exp\left[k(z-l)^2/2k_BT\right]\mathrm{d}y\\ &=\frac{1}{Z^{-}(c)}\sqrt{\frac{\pi k_BT}{2k}}\mathrm{erfi}\left[(c-l)\sqrt{\frac{k}{2k_BT}}\right]\end{aligned} \tag{22}$$

Finally, we obtain the detachment time of the link with one end tethered to a Gaussian chain confined outside of the sphere as:

$$\tau^{-} \approx \frac{Z^{-}(l)}{Z^{-}(c)}T \tag{23}$$

and

$$T = \frac{\pi k_BT}{2Dk}\mathrm{erfi}\left[(c-l)\sqrt{\frac{k}{2k_BT}}\right]\left[1+\mathrm{erf}\left(l\sqrt{\frac{k}{2k_BT}}\right)\right] \tag{24}$$

Similarly, the mean detachment time inside the sphere can be written as:

$$\tau^{+} \approx \frac{Z^{+}(l)}{Z^{+}(c)}T \tag{25}$$

where T is the product of Eqs. (21) and (22) after extracting the partition function and can be regarded as the mean exit time for the Brownian particle in a harmonic system.[26,38,47] The analytic approximation of this harmonic system can be written as:

$$\tau_0 = \frac{(c-l)^2}{D}\frac{\sqrt{\pi}\exp(\lambda)}{2\lambda^{3/2}},\ \lambda = \frac{k(c-l)^2}{2k_BT} \tag{26}$$

where τ_0 is the detachment time of a Brownian particle from a spring potential well under the influence of an entropic force approaching zero. In this case, τ_0 differs from the result unaffected by entropic forces by a factor of two. This is due to the fact that Brownian particle is much more likely to reach the right side of the spring potential well than the left one. We can derive the relationship between T and τ_0. Under the large-k assumption, $kl^2/2k_BT$ is much larger than 1, we can use the properties of the error function to get $\mathrm{erf}\left(\sqrt{kl^2/2k_BT}\right)\to1$. And for the imaginary error function, the approximate solution can be obtained by asymptotic expansion:[49]

$$\mathrm{erfi}(x) = -i\mathrm{erf}(ix) \approx -i\left[1-\frac{\exp\left(-x^2\right)}{\sqrt{\pi}}\left(\frac{1}{ix}-\frac{1}{2i^3x^3}\right)\right] \tag{27}$$

using the above equation, we can get

$$T \approx \frac{(c-l)^2}{D}\frac{\sqrt{\pi}\exp(\lambda)}{2\lambda^{3/2}}\left(1+\frac{1}{2\lambda}\right) = \left(1+\frac{1}{2\lambda}\right)\tau_0 \tag{28}$$

Under the large-k assumption, $1/(2\lambda)\to0$, it follows that $T\approx\tau_0$.

In Fig. 3 we give a comparison of the breakable link detachment times both inside and outside under spherical confinement with different stiffness constants k. We keep other parameters such as sphere radius R and the number of chain segments N constant and compare the difference in the mean detachment time between confining inside (dashed line) and outside (solid line) the sphere. Our results reveal that the breakable link inside the sphere is more likely to rupture than

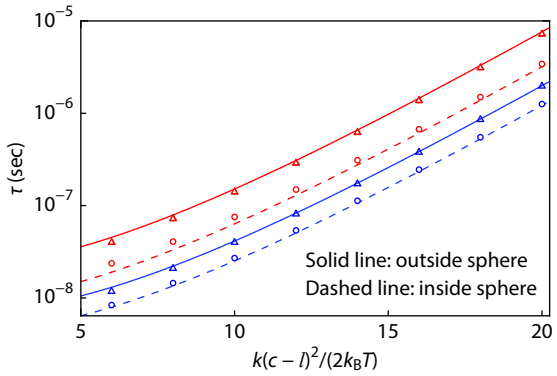

Fig. 3 Comparison of approximate and numerical calculations where l=b=2 nm, N=3 and R=10 nm. The blue and red colors indicate different breakable distances c=4 nm and c=6 nm. The solid and dashed lines produce the approximate expressions of Eqs. (23) and (25), while markers (circles and triangles) are the corresponding numerical results estimated from Eq. (19).

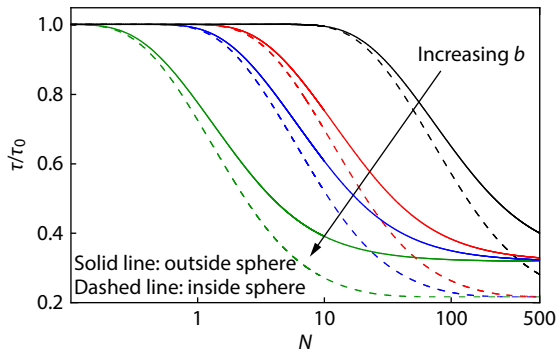

Fig. 4 Normalized detachment time τ/τ_0 of the flexible chain as a function of the number of chain segments N. Different values of b/l=0.2, 0.5, 0.7 and 1.5 (increasing along the arrow) are indicated by different colors. The solid lines represent the polymer chain confined outside of the sphere, while the dashed lines indicate the chain confined inside the sphere.

it is confined outside the sphere. We also give in Fig. 3 the numerical solution of the integral in Eq. (19) compared to the approximate solution in Eqs. (23) and (25). Our results demonstrate that the approximate calculation can be well-matched with the numerical calculation in large spring constant $k \geq 5k_BT$.

$\tau^{\pm}$ also related to the length of tethered polymer chain. In Fig. 4 we give the normalized $\tau^{\pm}$ change with the number of chain segments N. In order to enhance the impact of graph changes at different values of b, we increase the c/l ratio and keep c=4 nm, while set other parameters as l=1 nm, R=10 nm, and $k(c-l)^2/2 = 15k_BT$. According to Eq. (28) we realize that the entropic repulsion effect of the detached chain is reflected in the ratio of the partition functions, $\tau/\tau_0 \approx Z(l)/Z(c)$. The ratio of τ/τ_0 is 1 when N=0 (*i.e.*, without any detached chain), corresponding to the case of only spring potential well. And $\tau^{\pm}$ decreases rapidly and stabilizes as the number of monomers N increases. This suggests that increasing chain length significantly accelerates link rupture. We also found that the mean detachment time inside the sphere decreases more rapidly with increasing chain length and the stabilized value is smaller than that outside the sphere. This is because fewer conformations can be reached inside the sphere, resulting in a greater entropic force stretching the spring for the same chain length. In the next section, we will analyze the reasons for the different detachment times from the entropic force perspective.

INVESTIGATIONS OF ENTROPIC FORCE

In comparison to free polymers, the conformational entropy of the polymer is reduced when it is constrained by confinement. The reduction in entropy leads to additional entropic force. This force applied to the spring makes it easier for the chain to be detached from the substrate surface (as shown in Fig. 5). The entropic force on the polymer under confinement is typically calculated by taking a derivative of the free energy difference with respect to ξ in the direction of the radius of the sphere:

$$f = -\frac{\partial V_E}{\partial \xi} \tag{29}$$

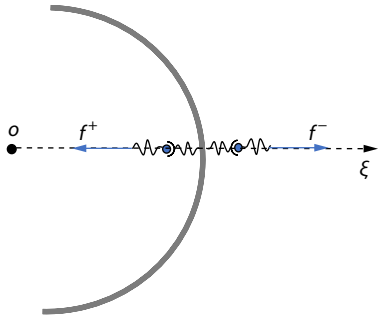

Fig. 5 Entropic forces exerted by polymer chains on springs.

As shown in Fig. 5, the spring extends in the same direction as the positive axis of the coordinate axes outside the sphere and in the opposite direction inside the sphere. Therefore, combining Eqs. (2), (10), (11) and (29), we obtain the expression for the entropic forces outside the sphere:

$$\begin{aligned} f^-(\xi) &= -\frac{\partial V_E^-}{\partial \xi} \\ &= k_BT\left\{\frac{1 + R\exp\left(-\xi^2/4R_g^2\right)/\left(R_g\sqrt{\pi}\right)}{\xi + R\mathrm{erf}\left[\xi/2R_g\right]} - \frac{1}{R+\xi}\right\} \end{aligned} \tag{30}$$

When the polymer is tethered inside the sphere, the directions of the polymer and the spring are opposite to the radial direction, resulting in a negative value for ξ. The entropic force of the polymer inside the sphere can be expressed as:

$$\begin{aligned} f^+(\xi) &= -\frac{\partial \Delta V_E^+}{\partial \xi} \\ &= k_BT\left\{\frac{\pi}{R}\frac{\sum_{m=1}^{\infty}(-1)^{1+m}\exp\left(-R_g^2m^2\pi^2/R^2\right)\cos\left[m\pi(R-\xi)/R\right]}{\sum_{m=1}^{\infty}(-1)^{1+m}\exp\left(-R_g^2m^2\pi^2/R^2\right)\sin\left[m\pi(R-\xi)/R\right]/m} - \frac{1}{R-\xi}\right\} \end{aligned} \tag{31}$$

Eqs. (30) and (31) provide the analytical expression for the surface entropic force averaged over all possible configurations of the Gaussian chain. The surface force depends on the tethering position ξ, the radius of the sphere R, and the gyra-

tion radius R_g of the chain.

The entropic force inside the sphere is negative, while it is positive outside the sphere. As shown in Fig. 6, we represent the absolute value of the entropic forces both inside and outside the sphere as a function of the parameters N. Both forces are applied to the chain by the wall and drive the chain away from the confining surface, which accelerates the detachment of the polymer from the surface. Comparing Figs. 6(a) with 6(b), we can see that the entropic force inside the sphere is larger than outside the sphere for the same model parameters. This is the reason for the difference in the mean detachment time of the link. For a sufficiently long chain, the entropic force reaches a plateau. The entropic force inside the sphere f^+ is dominated by the first term (m=1) in Eq. (31). We can estimate the limit value of the entropic force acting on the polymer by the wall as:

$$f^+(\xi, N\to\infty) = k_BT\left[\frac{\pi\cot\left[\pi(R-\xi)/R\right]}{R} - \frac{1}{R-\xi}\right] \tag{32}$$

And the expression of the entropic force outside the sphere can be expressed as:

$$f^-(\xi, N\to\infty) = k_BT\left(\frac{1}{\xi} - \frac{1}{R+\xi}\right) \tag{33}$$

It is apparent that the entropic force is no longer dependent on the chain length but only relates to the chain's one end location distance from the wall ξ and radius of the sphere.

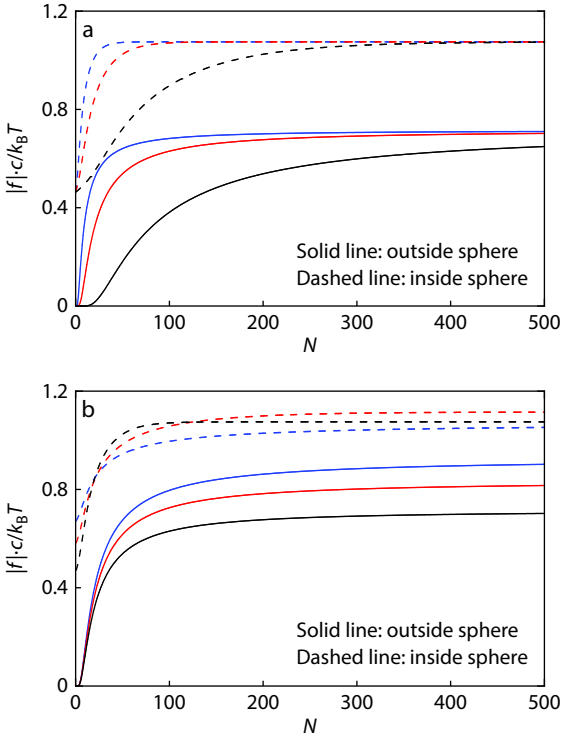

Fig. 6 Entropic force exerted on the chain by the sphere surfaces with different numbers of chain segments N. We set spring initial length l=1 nm and the link-breaking distance c=4 nm. The solid lines represent the polymer chain confined outside of the sphere, while the dashed lines indicate the chain confined inside the sphere. (a) Different segment lengths b/l=0.5 (black), 1 (blue), and 1.5 (red); (b) Different sphere radius R=10 nm (black), 20 nm (blue), and 50 nm (red).

In Fig. 7, we compare the entropic force when the polymer is tethered on the flat wall, outside the sphere, and inside the sphere with increasing chain length. The entropic force of the polymer chain tethered at a distance ξ from flat wall can be written as:[44]

$$f_0(\xi) = k_BT\frac{\exp\left[-\xi^2/(2R_g)^2\right]}{\sqrt{\pi}R_g\,\mathrm{erf}\left(\xi/2R_g\right)} \tag{34}$$

as $N\to\infty$

$$f_0(\xi, N\to\infty) = -k_BT/\xi \tag{35}$$

We find that the entropic forces from largest to smallest are f^+, f_0 and f^-. The largest entropic force makes the breakable link inside the sphere with one end tethered to a polymer chain the fastest to reach the rupture distance $\xi = c$, which implies the minimum mean detachment time.

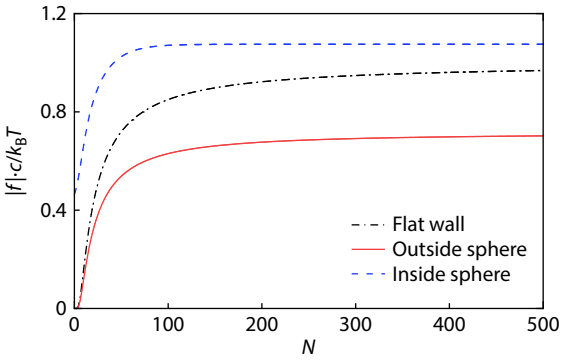

Fig. 7 Comparison of entropic force exerted on the chain by flat wall and spherical surface as a function of the number of chain segments N. The spring initial length and the segment length are l=b= 1 nm and the link-breaking distance c=4 nm. The sphere radius is R=10 nm.

CONCLUSIONS AND DISCUSSION

In this study, we studied the step-by-step detachment kinetics of polymer chains in a spherical substrate. The spherical face geometry constraint and the long polymer chains made the breakable links subject to additional wall-imposed entropic forces that changed the height of the energy potential barrier. The MFPT method was used to calculate how the entropic repulsion given by spherical confinement affects the mean detachment time of the breakable link. Compared to the simple spring potential energy, the entropy effect reduces the mean detachment time of the links inside and outside the sphere, and the time is related to the partition function $Z^{\pm}(l)/Z^{\pm}(c)$. And we found that the link inside the sphere is more easily ruptured due to the different boundary conditions inside and outside the sphere that make the Gaussian chain configuration distribution different, leading to stronger repulsion of the chain on the inside wall of the sphere. Compared with the entropic force f_0 of the flat wall confinement, the entropic force inside the sphere $f^+ > f_0$ while the entropic force outside the sphere $f^- < f_0$. As the chain length increases, the entropic force and detachment time will gradually approach a plateau and only relate to the distance ξ and radius of the sphere R.

https://doi.org/10.1007/s10118-023-3049-5

This work investigated the detachment kinetics of polymer chains on the surface of a sphere by means of a simple ideal Gaussian chain model. The excluded volume effect and the bending stiffness of the polymer chains, which were important in the dissociation problem, were not considered here and will be refined in the subsequent work.

APPENDIX: DERIVATION OF $Z^{\pm}$

Derivation of Z^{+}

In this section, we calculate the partition function for a polymer chain inside a sphere with one end anchored to a breakable link at $\mathbf{r} = (R - \xi, 0, 0)$. In our model, we assume the spring's elongation restrict in the radial direction. The other free end of the polymer can be at any position $\mathbf{r'}$ inside the sphere. The full solution of the Green's function in the spherical coordinate system can be written as:[42,44]

$$G^{+}(\mathbf{r}, \mathbf{r'}, N) = \frac{1}{2\pi R^2\sqrt{rr'}}\sum_{n=0}^{\infty}\sum_{\beta}(2n+1)P_n(\cos\gamma) \frac{J_{n+(1/2)}\left(\beta\frac{r}{R}\right)J_{n+(1/2)}\left(\beta\frac{r'}{R}\right)}{\left(J'_{n+(1/2)}(\beta)\right)^2}\exp\left(-\frac{\beta^2 Nb^2}{6R^2}\right) \tag{A1}$$

$P_n(\cos\gamma)$ are the Legendre polynomials of order n, J_v are the Bessel functions of the first kind of order v and β are the various zeroes of $J_{n+(1/2)}(\beta)$

$$J_{n+(1/2)}(\beta) = 0 \tag{A2}$$

Integration over the position of the free end $\mathbf{r'}$ yields

$$Z^{+} = \int_0^{2\pi} \mathrm{d}\phi \int_0^{\pi} \mathrm{d}\gamma \sin(\gamma) \int_0^{R} r'^2 \mathrm{d}r' G^{+}(\mathbf{r}, \mathbf{r'}, N) \tag{A3}$$

This integral can be simplified by the orthogonality of the Legendre polynomials $P_n(\cos\gamma)$:

$$\int_0^{\pi} P_i(\cos\gamma) P_j(\cos\gamma)\mathrm{d}\cos\gamma = \begin{cases} \frac{2}{2i+1}, & i = j \\ 0, & i \neq j \end{cases} \tag{A4}$$

This allows us to keep only the terms with n=0 in the expression for Eq. (A1). Thus, the Green's function in Eq. (A3) can be written as

$$G^{+}(\mathbf{r}, \mathbf{r'}, N) = \frac{1}{2\pi R^2\sqrt{rr'}}\sum_{\beta}P_0(\cos\gamma) \frac{J_{1/2}\left(\beta\frac{r}{R}\right)J_{1/2}\left(\beta\frac{r'}{R}\right)}{\left(J'_{1/2}(\beta)\right)^2}\exp\left(-\frac{\beta^2 Nb^2}{6R^2}\right) \tag{A5}$$

where $\beta = m\pi$ (m=1, 2,……) is the roots of $J_{1/2}(\beta) = 0$, and the sum over β in Eq. (A5) indicates the summation over these roots.

Herein, we can already see that the calculation of the partition function is independent of the angle according to $P_0(\cos\gamma)$=1. Substituting Eq. (A5) into Eq. (A3), we get

$$Z^{+} = \frac{2}{R^2\sqrt{r}}\sum_{m=1}^{\infty}\int_0^{R}(r')^2\frac{1}{\sqrt{r'}}J_{1/2}\left(\beta\frac{r'}{R}\right)\mathrm{d}r' \times \frac{J_{1/2}\left(\beta\frac{r}{R}\right)}{\left[J'_{1/2}(\beta)\right]^2}\exp\left(-\frac{m^2\pi^2 R_g^2}{R^2}\right) \tag{A6}$$

Calculating the integral in Eq. (A6) by using $\int_0^1 x^{v+1}J_v(ax)\mathrm{d}x = a^{-1}J_{v+1}(a)$ yields:[49]

$$I = \int_0^{R}(r')^2\frac{1}{\sqrt{r'}}J_{1/2}\left(\beta\frac{r'}{R}\right)\mathrm{d}r' = R^{5/2}\frac{1}{\beta}J_{3/2}(\beta) \tag{A7}$$

Then, we give the definition of the Bessel function

$$\begin{aligned} J_{1/2}(x) &= \sqrt{\frac{2}{\pi x}}\sin x \\ J_{3/2}(x) &= \sqrt{\frac{2}{\pi x}}\left(\frac{\sin x}{x} - \cos x\right) \\ J'_{1/2}(x) &= \sqrt{\frac{2}{\pi x}}\left(-\frac{1}{2}\frac{\sin x}{x} + \cos x\right) \end{aligned} \tag{A8}$$

Substituting $r = R - \xi$, Eqs. (A7) and (A8) into Eq. (A6) gives an expression for the partition function of the polymer chain inside the sphere as:

$$Z^{+} = \frac{2R}{\pi(R-\xi)}\sum_{m=1}^{\infty}\frac{(-1)^{m+1}}{m}\sin\left[\frac{m\pi(R-\xi)}{R}\right] \times \exp\left(-\frac{m^2\pi^2 R_g^2}{R^2}\right) \tag{A9}$$

Derivation of Z^{-}

Now we consider a polymer chain with one end anchored to a breakable link located at $\mathbf{r} = (R + \xi, 0, 0)$ outside a sphere. The other end $\mathbf{r'}$ is free in space outside the sphere confinement. The Green's function can be expressed as:[42]

$$G^{-}(\mathbf{r}, \mathbf{r'}, N) = \frac{1}{4\pi\sqrt{rr'}}\sum_{n=0}^{\infty}(2n+1)P_n(\cos\gamma) \int_0^{\infty}\frac{C_{n+(1/2)}(ur)C_{n+(1/2)}(ur')}{J^2_{n+(1/2)}(uR) + Y^2_{n+(1/2)}(uR)}e^{-Nb^2u^2/6}u\mathrm{d}u \tag{A10}$$

with $C_{n+(1/2)}(z) = J_{n+(1/2)}(z)Y_{n+(1/2)}(uR) - Y_{n+(1/2)}(z)J_{n+(1/2)}(uR)$. Y_v are the Bessel functions of the second kind of order v. Similar to the previous procedure in the calculation of Z^{+}, the Green's function in Eq. (A10) can still retain only the n=0 terms as:

$$G^{-}(\mathbf{r}, \mathbf{r'}, N) = \frac{1}{4\pi\sqrt{rr'}}\int_0^{\infty}\frac{C_{1/2}(ur)C_{1/2}(ur')}{J^2_{1/2}(uR) + Y^2_{1/2}(uR)} \times \exp\left(-\frac{Nb^2u^2}{6}\right)u\mathrm{d}u \tag{A11}$$

where $Y_{1/2}(z) = J_{-1/2}(z) = \sqrt{2/(\pi z)}\cos z$. Substituting Eq. (A8) into Eq. (A11), we can get

$$G^{-}(\mathbf{r}, \mathbf{r'}, N) = \frac{1}{2\pi^2 rr'}\int_0^{\infty}\sin\left[u(r-R)\right] \sin\left[u(r'-R)\right]\exp\left(-\frac{Nb^2u^2}{6}\right)\mathrm{d}u \tag{A12}$$

The Green's function of the polymer chain outside the sphere is calculated for the integral as:

$$G^{-}(\mathbf{r}, \mathbf{r'}, N) = \frac{1}{8\pi rr'\sqrt{\pi Nb^2/6}}\left\{\exp\left[-\frac{3(r'-r)^2}{2Nb^2}\right] -\exp\left[-\frac{3(r'+r-2R)^2}{2Nb^2}\right]\right\} \tag{A13}$$

then the partition function of the polymer chain outside the sphere can be obtained as:

$$Z^{-} = \int_0^{2\pi} d\phi \int_0^{\pi} d\gamma \sin(\gamma) \int_R^{\infty} r'^2 dr' G^{-}(\mathbf{r}, \mathbf{r}', N) = \frac{\xi + R \cdot \mathrm{erf}\left(\xi / 2R_g\right)}{R + \xi} \quad \text{(A14)}$$

In conclusion, we derived the partition function $Z^{\pm}$ of the polymer inside and outside the sphere from the full solution of the Green's function $G^{\pm}$. The calculation of $Z^{\pm}$ can also be found in some other literature consistent with our calculation process.[44,50,51]

Conflict of Interests

The authors declare no interest conflict.

ACKNOWLEDGMENTS

This work was financially supported by the National Natural Science Foundation of China (No. 51965057), Xinjiang Tianchi PhD Project (No. TCBS202113), the Natural Science Foundation of Xinjiang (No. 2022D01C34), Xinjiang Basic Research Funds for Universities (No. XJEDU2022P017), Robot-Intelligent Equipment Technology Innovation (No. 2022D14002) and Xinjiang Tianshan Science Technology Innovation Leading Talents Program (No. 2022TSYCLJ0044).

REFERENCES

1 Claesson, P. M.; Blomberg, E.; Fröberg, J. C.; Nylander, T.; Arnebrant, T. Protein interactions at solid surfaces. *Adv. Colloid Interface Sci.* **1995**, *57*, 161–227.
2 Lipowsky, R. Flexible membranes with anchored polymers. *Colloids Surf. A* **1997**, *128*, 255–264.
3 Ayscough, K. R. *In vivo* functions of actin-binding proteins. *Curr. Opin. Cell Biol.* **1998**, *10*, 102–111.
4 Smith, D. E.; Tans, S. J.; Smith, S. B.; Grimes, S.; Anderson, D. L.; Bustamante, C. The bacteriophage φ29 portal motor can package DNA against a large internal force. *Nature* **2001**, *413*, 748–752.
5 Aliee, M.; Najafi, A. Mechanical properties of an adsorbed elastic polymer in contact with a rigid membrane. *Phys. Rev. E* **2008**, *78*, 051802.
6 Paturej, J.; Dubbeldam, J. A.; Rostiashvili, V. G.; Milchev, A.; Vilgis, T. A. Force spectroscopy of polymer desorption: theory and molecular dynamics simulations. *Soft Matter* **2014**, *10*, 2785–2799.
7 Chaudhuri, A.; Chaudhuri, D. Forced desorption of semiflexible polymers, adsorbed and driven by molecular motors. *Soft Matter* **2016**, *12*, 2157–2165.
8 Li, B.; Abel, S. M. Shaping membrane vesicles by adsorption of a semiflexible polymer. *Soft Matter* **2018**, *14*, 185–193.
9 Saltzman, W. M.; Kyriakides, T. R. Cell interactions with polymers. In *Principles of Tissue Engineering*. 4th Ed. Academic Press, **2020**, 275–293.
10 Lee, J. H.; Gustin, J. P.; Chen, T. Vesicle-biopolymer gels: Networks of surfactant vesicles connected by associating biopolymers. *Langmuir* **2005**, *21*, 26–33.
11 Skulason, H.; Frisbie, C. D. Direct detection by atomic force microscopy of single bond forces associated with the rupture of discrete charge-transfer complexes. *J. Am. Chem. Soc.* **2002**, *124*, 15125–15133.
12 Stout, A. L. Detection and characterization of individual intermolecular bonds using optical tweezers. *Biophy. J.* **2001**, *80* 2976–2986.
13 Hanke, F.; Livadaru, L.; Kreuzer, H. J. Adsorption forces on a single polymer molecule in contact with a solid surface. *Europhys. Lett.* **2005**, *69*, 242–248.
14 Kierfeld, J. Force-induced desorption and unzipping of semiflexible polymers. *Phys. Rev. Lett.* **2006**, *97*, 058302.
15 Essevaz-Roulet, B.; Bockelmann, U.; Heslot, F. Mechanical separation of the complementary strands of DNA. *Proc. Natl. Acad. Sci. U. S. A.* **1997**, *94*, 11935–11940.
16 Cocco, S.; Monasson, R.; Marko, J. F. Force and kinetic barriers to unzipping of the DNA double helix. *Proc. Natl. Acad. Sci. U. S. A.* **2001**, *98*, 8608–8613.
17 Zou, S.; Schönherr, H.; Vancso, G. J. Stretching and rupturing individual supramolecular polymer chains by AFM. *Angew. Chem.* **2005**, *44*, 978–981.
18 Hugel, T.; Grosholz, M.; Clausen, S. H.; Pfau, A.; Gaub, H.; Seitz, M. Elasticity of single polyelectrolyte chains and their desorption from solid supports studied by AFM based single molecule force spectroscopy. *Macromolecules* **2001**, *34*, 1039–1047.
19 Benetatos, P.; Frey, E. Depinning of semiflexible polymers. *Phys. Rev. E* **2003** , *67*, 051108.
20 Florio, G.; Puglisi, G.; Giordano, S. Role of temperature in the decohesion of an elastic chain tethered to a substrate by onsite breakable links. *Phys. Rev. Res.* **2020**, *2*, 033227.
21 Paturej, J.; Milchev, A.; Rostiashvili, V. G.; Vilgis, T. A. Polymer detachment kinetics from adsorbing surface: theory, simulation and similarity to infiltration into porous medium. *Macromolecules* **2012**, *45*, 4371–4380.
22 Singh, N.; Singh, Y. Statistical theory of force-induced unzipping of DNA. *Eur. Phys. J. E* **2005**, *17*, 7–19.
23 Jánosi, I. M.; Chrétien, D.; Flyvbjerg, H. Structural microtubule cap: stability, catastrophe, rescue, and third stat. *Biophys. J.* **2002**, *83*, 1317–1330.
24 Kallrot, N.; Linse, P. Dynamic study of single-chain adsorption and desorption. *Macromolecules* **2007**, *40*, 4669–4679.
25 Zhao, S. L.; Wu, J.; Gao, D.; Wu, J. Z. Gaussian fluctuations in tethered DNA chains. *J. Chem. Phys.* **2011**, *134*, 065103.
26 Lee, C. T.; Terentjev, E. M. Hard-wall entropic effect accelerates detachment of adsorbed polymer chains. *Phys. Rev. E* **2019**, *100*, 032501.
27 Schweizer, K. S.; Saltzman, E. J. Entropic barriers, activated hopping, and the glass transition in colloidal suspensions. *J. Chem. Phys.* **2003**, *119*, 1181–1196.
28 Wozinski, A.; Iwaniszewski, J. Relaxation through an asymmetric fluctuating potential barrier. *Phys. Rev. E* **2009**, *80*, 011129.
29 Fiasconaro, A.; Spagnolo, B. Resonant activation in piecewise linear asymmetric potentials. *Phys. Rev. E* **2011**, *83*, 041122.
30 Hummer, G.; Szabo, A. Kinetics from nonequilibrium single-molecule pulling experiments. *Biophys. J.* **2003**, *85*, 5–15.
31 Frantz, P.; Granick, S. Kinetics of polymer adsorption and desorption. *Phys. Rev. Lett.* **1991**, *66*, 899–902.
32 Frantz, P.; Granick, S. Exchange kinetics of adsorbed polymer and the achievement of conformational equilibrium. *Macromolecules* **1994**, *27*, 2553–2558.
33 Goeler, F. V.; Muthukumar, M. Adsorption of polyelectrolytes onto curved surfaces. *J. Chem. Phys.* **1994**, *100*, 7796–7803.
34 Ball, R. C.; Blunt, M.; Barford, W. Can surface bound states be induced by interfacial roughness? *J. Phys. A.* **1989**, *22*, 2587–2595.
35 Moore, N. W.; Kuhl, T. L. The role of flexible tethers in multiple ligand-receptor bond formation between curved surfaces. *Biophys. J.* **2006**, *91*, 1675–1687.
36 Tanaka, M.; Sackmann E. Polymer-supported membranes as models of the cell surface. *Nature* **2005**, *437*, 656–663.
37 Hänggi, P.; Talkner, P.; Borkovec, M. Reaction-rate theory: fifty

years after kramers. *Rev. Mod. Phys.* **1990**, *62*, 251–341.
38 Risken, H. *The Fokker-Planck equation*. Springer, Berlin, Heidelberg, **1996**, Vol.18.
39 Chen, Z. J. Theory of wormlike polymer chains in confinement. *Prog. Polym. Sci.* **2016**, *54*, 3–46.
40 Doi, M.; Edwards. S. F. *The theory of polymer dynamics*. Oxford University Press, **1988**, Vol. 73.
41 Cole, K.; Beck, J.; Haji-Sheikh A Heat conduction using Green's function. *Scitech Book News*. **2010**, Vol. 34.
42 Carslaw, H. S.; Jaeger, J. C. *Conduction of heat in solids*. Oxford University Press, **1959**.
43 Muthukumar, M. Polymers under confinement. *Adv. Chem. Phys.* **2012**, *149*, 129–196.
44 Dutta, S.; Benetatos, P. Statistical ensemble inequivalence for flexible polymers under confinement in various geometries. *Soft Matter* **2020**, *16*, 2114–2127.
45 VanBuren, V.; Odde, D. J.; Cassimeris, L. Estimates of lateral and longitudinal bond energies within the microtubule lattice. *Proc. Natl. Acad. Sci. U. S. A.* **2002**, *99*, 6035–6040.
46 Zakharov, P.; Gudimchuk, N.; Voevodin, V.; Tikhonravov, A.; Ataullakhanov, F. I.; Grishchuk, E. L. Molecular and mechanical causes of microtubule catastrophe and aging. *Biophys. J.* **2015**, *109*, 2574–2591.
47 Grebenkov, D. S. First exit times of harmonically trapped particles: a didactic review. *J. Phys. A: Math. Theor.* **2015**, *48*, 013001.
48 Pavliotis, G. A. *Stochastic processes and applications: diffusion processes, the Fokker-Planck and Langevin equations*. Springer, Berlin, **2014**.
49 Gradshteyn, I. S.; Ryzhik, I. M. *Table of integrals, series, and products*. Academic Press, **2014**.
50 Hiergeist, C.; Lipowsky, R. Elastic properties of polymer-decorated membranes. *J. Phys. II* **1996**, *6*, 1465–1481.
51 Park, J. P.; Sung, W. Polymer release out of a spherical vesicle through a pore. *Phys. Rev. E* **1998**, *57*, 730–734.

https://doi.org/10.1007/s10118-023-3049-5